

Liquid Oxygen Cooling of Hydrocarbon Fueled Rocket Thrust Chambers

Elizabeth A. Roncace*

NASA Lewis Research Center, Cleveland, Ohio 44135

Rocket engines using liquid oxygen (LOX) and hydrocarbon fuel as the propellants are being given serious consideration for future launch vehicle propulsion. Normally, the fuel is used to regeneratively cool the combustion chamber. However, hydrocarbons such as RP-1 are limited in their cooling capability. Another possibility for the coolant is the liquid oxygen. Combustion chambers previously tested with LOX and RP-1 as propellants and LOX as the coolant have demonstrated the feasibility of using liquid oxygen as a coolant up to a chamber pressure of 13.8 MPa (2000 psia). However, there has been concern as to the effect on the integrity of the chamber liner if oxygen leaks into the combustion zone through fatigue cracks that may develop between the cooling passages and the hot-gas-side wall. In order to study this effect, chambers were fabricated with slots machined upstream of the throat between the cooling passage wall and the hot-gas-side wall to simulate cracks. The chambers were tested at a nominal chamber pressure of 8.6 MPa (1247 psia) over a range of mixture ratios from 1.5 to 3.1 using liquid oxygen as the coolant. The results of the testing showed that the leaking LOX did not have a deleterious effect on the chambers, i.e., there was no evidence of melting in the region of the slots or of the wall reaching its ignition temperature. However, there was melting in the throat region of two chambers but not in line with the slots. The cause of the melting was thoroughly investigated and was determined to be a result of injector anomalies.

Introduction

PRELIMINARY design studies^{1,2} for future space transportation systems have shown a benefit for high pressure booster engines using liquid oxygen (LOX) and a hydrocarbon fuel as the propellants. The candidate hydrocarbon fuels for future launch systems are RP-1, propane and methane.

When cooling a high pressure rocket thrust chamber, the fuel in a rocket engine is typically used to regeneratively cool the combustion chamber. The disadvantage of RP-1, and even the lighter paraffinic hydrocarbon propane, is decomposition (coking) in the cooling passages and corrosion of the copper wall by trace amounts of sulfur-containing compounds. However, recent testing³ has shown that RP-1 and methane can be used as coolants at coolant-side wall temperatures up to 304°C (580°F) and 499°C (930°F), respectively, without coking or corrosion if there are no sulfur-containing compounds present.

Because of the problems associated with hydrocarbon regenerative cooling, liquid oxygen is being considered as an alternative coolant. There are two concerns with LOX as a coolant: 1) its heat transfer capability and 2) the effect of leakage into the combustion zone if cracks develop in the chamber liner. Analyses^{1,4} and experimental work⁵⁻⁷ have shown that oxygen can cool rocket engines at chamber pressures up to 27.6 MPa (4000 psia) and 13.8 MPa (2000 psia), respectively, and still maintain reasonable pressure drops. In the experimental work fatigue cracks, similar to those that develop with fuel cooling, developed in the throat regions at chamber pressures of 4.1 MPa (600 psia) and 8.6 MPa (1250

psia) and the leaking LOX coolant had no effect on the chamber wall. However, there was still some concern as to whether oxygen leaking through cracks between the injector and the throat, where the boundary layer has not been fully developed and there is still combustion occurring, would affect the integrity of the thrust chamber.

The objective of this program was to evaluate the effect of oxygen leaking into the combustion zone through cracks upstream of the thrust chamber throat and to acquire more experience using liquid oxygen as a coolant. Three thrust chambers had slots machined upstream of the throat between the cooling passage wall and the hot-gas-side wall to simulate cracks. A fourth chamber was built without slots for comparison purposes. These LOX-cooled thrust chambers were tested at a nominal chamber pressure of 8.6 MPa (1247 psia) at oxygen-to-fuel mixture ratios from 1.5 to approximately 3.1.

Apparatus

The hardware used for this program consisted of two 61-element injectors, several resonators, and four combustion

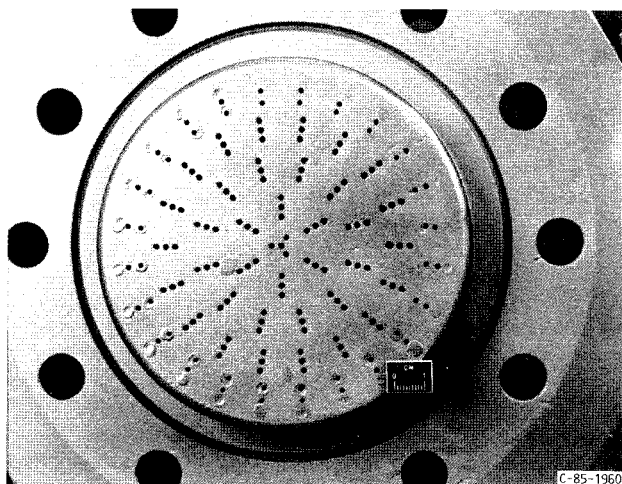


Fig. 1 61 Element triplet injector.

Presented as Paper 89-2739 at the AIAA/ASME/SAE/ASEE 25th Joint Propulsion Conference, Monterey, CA, July 10-12, 1989; received Oct. 6, 1989; revision received Aug. 3, 1990; accepted for publication Jan. 7, 1991. Copyright © 1989 by the American Institute of Aeronautics and Astronautics, Inc. No copyright is asserted in the United States under Title 17, U.S. Code. The U.S. Government has a royalty-free license to exercise all rights under the copyright claimed herein for Governmental purposes. All other rights are reserved by the copyright owner.

*Aerospace Engineer, Launch Vehicle Technology Branch. Member AIAA.

Table 1 Injector geometry of 61-element injector with triplet oxygen-fuel-oxygen tangential liquid oxygen fans

| Hole diameter, mm (in.) | | | Flow area, mm ² (in. ²) | | | Total flow area, mm ² (in. ²) | Portion of total flow in outer zone, percent | Nominal chamber pressure, P _c , MPa abs (psia) |
|-------------------------|------------------|------------------|--|---------------------|---------------------|--|--|---|
| Outer zone | Core zone | Center zone | Outer zone, 24 holes | Core zone, 36 holes | Center zone, 1 hole | | | |
| Fuel element | | | | | | | | |
| 1.168 (0.046) | 1.600 (0.063) | 1.600 (0.063) | 25.715 (0.040) | 72.382 (0.112) | 2.011 (0.0031) | 100.111 (0.1551) | 25.7 | 8.6 (1247) |
| Oxidizer element | | | | | | | | |
| 1.168 (0.046) | 1.702 (0.067) | 1.397 (0.055) | 25.735 (0.040) | 163.74 (0.254) | 4.581 (0.0071) | 194.05 (0.3011) | 13.2 | 8.6 (1247) |

chambers. Three of the chambers had two slots machined through the wall between the cooling channels and the hot-gas side, while the fourth chamber was fabricated without slots.

Injector

Figure 1 shows a 61-element triplet injector with 4 radial rings of elements and a central quad element that provided 3 oxidizer streams impinging on a straight fuel stream. The three innermost radial rings were arranged in an oxidizer-fuel-oxidizer (O-F-O) sequence to provide good propellant mixing, fuel vaporization, and mass flux distribution. The outermost radial ring consisted of F-O doublet showerheads to provide more fuel in the outer zone, which resulted in fuel film cooling of the chamber wall.

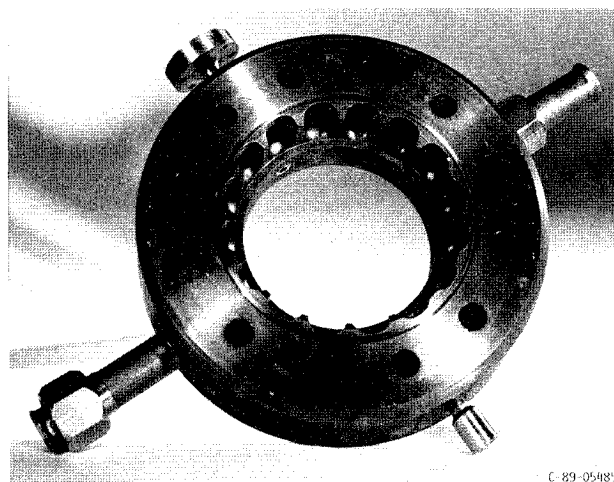
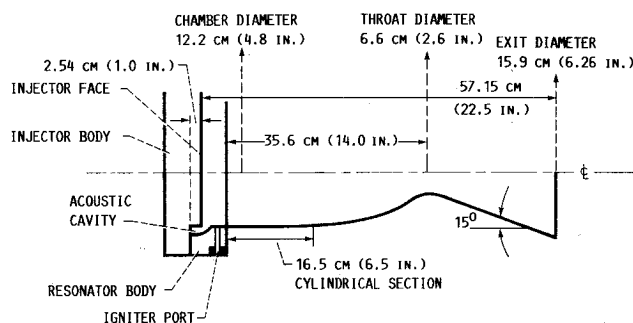
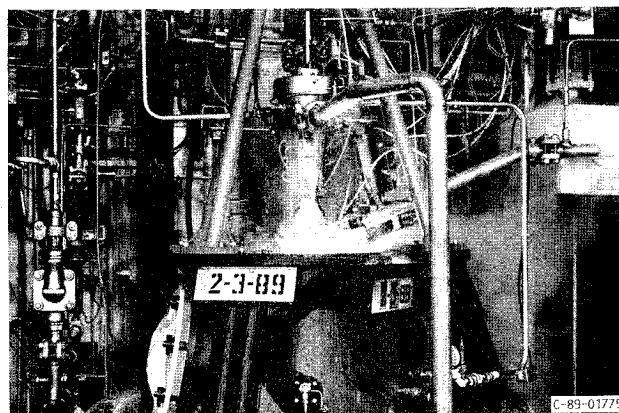
The first injector, injector 288, used in this program was originally fabricated with 61 elements as triplets arranged in a pattern to provide LOX tangential fans. Because this pattern had resulted in high temperatures at the gas wall (Ref. 4), the injector was modified in the outer ring of elements by welding all the holes closed and then redrilling as F-O doublet showerheads. The use of this injector in the present program resulted in oxygen-rich streaks on the chamber wall and non-uniform mixing in the combustion zone. The streaking did not appear to be a function of the mixture ratio, as the streaks occurred at operating conditions above and below the stoichiometric mixture ratio. Injector 288 was water flowed after being tested with chambers 702 and 703, which showed that several of the oxygen element streams did not flow at the proper angle. The elements in the outer row of the new injector, injector 309, were drilled as showerheads and water-flow tests showed that all the oxygen element streams were properly aligned. Also, the hot-fire tests showed that there were no oxygen-rich streaks on the chamber wall and the mixing was uniform. More details of the injector are given in Table 1.

Resonator

A water-cooled resonator, as shown in Fig. 2, was used in this investigation to provide stable combustion. It was composed of 16 acoustic cavities arranged evenly around its inside surface. The resonator was placed between the chamber and the injector. The cavities were in line with the chamber at its edge and were 3.63 cm (1.43 in.) long. The injector formed the inner wall of the cavities which was 2.54 cm (1.0 in.) long. This corresponded to a quarter wave tube to dampen the second tangential frequency of 9700 cycles/s which was the expected frequency of the combustion oscillations driving the instability. A hydrogen-oxygen spark torch igniter was located in the resonator wall just downstream of the acoustic cavities.

Combustion Chamber

Figure 3 shows the dimensions of the combustion chambers used in this test program. The diameter of the cylindrical section is 12.19 cm (4.80 in.). At the throat section, the di-

**Fig. 2** Acoustic resonator.**Fig. 3** Combustion chamber dimensions.**Fig. 4** Chamber 702 during test firing.

ameter is 6.60 cm (2.60 in.), while the diameter at the nozzle exit is 15.90 cm (6.26 in.), for an exit area ratio of 5.80. The length from the injector face to the throat is 39.37 cm. (15.50 in.) and the distance from the throat to the exit plane is 17.78 cm. (7.00 in.). The hot-gas liners were fabricated from oxygen-free, high conductivity (OFHC) copper and contained 100 axial milled channels for the coolant passages. The passages were closed out with electroformed nickel.

Four combustion chambers were tested in this program. Chamber 702 is shown in Fig. 4 during a firing. To determine

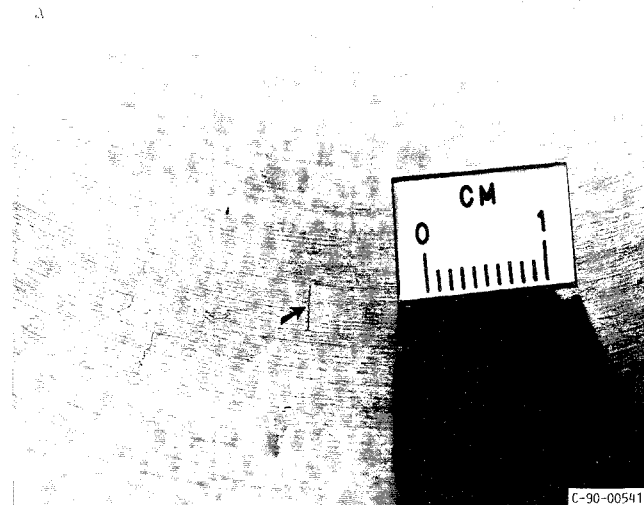


Fig. 5 Machined slot on chamber 704 after testing.

the effects of cracks occurring upstream of the throat, chambers 702, 703, and 704 were fabricated with two machined slots 180 deg apart. The machined slots were not in the same circumferential location in the chambers relative to the injector. Instead, the slots in chamber 702 were 45 deg off from those in chamber 703 and 704. The slots were 0.4 to 1.0 cm (0.16 to 0.40 in.) long and 0.0127 cm (0.005 in.) wide. Figure 5 shows a close-up view of one of the slots in chamber 704. From the continuity equation and assuming constant density across the slot, the leakage through the two slots is calculated to be 25% of the total coolant through a given channel, or an estimated 0.5% of the total coolant. Figure 6 shows the axial slot thermocouples imbedded in the rib between coolant channels approximately 1.30 mm (0.51 in.) from the hot-gas

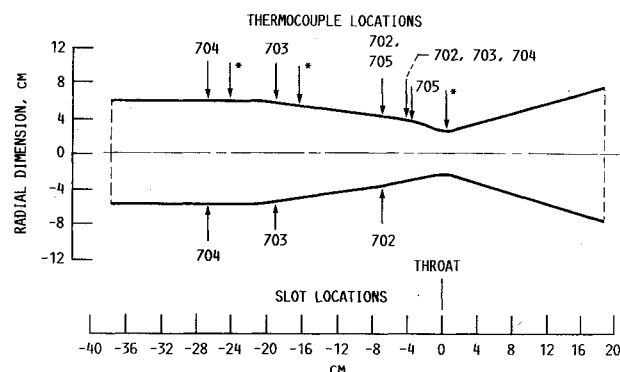


Fig. 6 Slot and thermocouple locations. Chamber number indicates which chamber had thermocouples or slots at the given location.

Table 2 Test conditions^a

| Run | Chamber | Chamber pressure | | Ratio of oxidant to fuel, O/F | Coolant flow rate | | Oxidant flow rate | | Characteristic exhaust velocity efficiency, C* |
|-----|---------|------------------|------|-------------------------------|-------------------|-------|-------------------|-------|--|
| | | MPa abs | psia | | kg/s | lbm/s | kg/s | lbm/s | |
| 22 | 702 | 8.32 | 1208 | 2.71 | 12.00 | 26.50 | 12.60 | 27.70 | 91.8 |
| 25 | 702 | 7.96 | 1155 | ^b 3.10 | 14.70 | 32.40 | 12.50 | 27.40 | 94 |
| 32 | 703 | 8.27 | 1200 | 2.58 | 14.10 | 31.10 | 12.50 | 27.40 | 90.6 |
| 33 | | 8.54 | 1239 | 2.78 | 14.40 | 31.80 | 12.60 | 27.80 | 94.8 |
| 34 | | 8.60 | 1247 | 2.72 | 14.30 | 31.50 | 11.60 | 25.50 | 95.5 |
| 35 | | 8.56 | 1241 | 2.33 | 14.20 | 31.20 | 11.60 | 25.60 | 96.5 |
| 36 | | 8.62 | 1250 | 1.91 | 13.90 | 30.70 | 11.00 | 24.30 | 97.8 |
| 38 | | 8.78 | 1273 | 2.18 | 13.60 | 30.00 | 11.50 | 25.30 | 98 |
| 58 | 705 | 8.15 | 1182 | 1.58 | 14.90 | 32.70 | 11.40 | 25.10 | 89.3 |
| 59 | | 8.54 | 1239 | 1.76 | 14.80 | 32.50 | 10.70 | 23.60 | 99.8 |
| 60 | | 8.66 | 1256 | 1.76 | 14.70 | 32.30 | 10.90 | 23.90 | 99.6 |
| 61 | | 9.01 | 1307 | 2.20 | 13.60 | 29.90 | 12.10 | 26.70 | 96.6 |
| 62 | | 8.89 | 1290 | 2.18 | 13.50 | 29.60 | 12.00 | 26.40 | 96.1 |
| 63 | | 8.62 | 1250 | 2.05 | 13.80 | 30.30 | 11.50 | 25.20 | 96 |
| 65 | | 8.37 | 1214 | 1.94 | 14.10 | 31.00 | 11.00 | 24.10 | 96.8 |
| 66 | | 8.36 | 1213 | 1.91 | 13.70 | 30.10 | 11.10 | 24.50 | 94.7 |
| 75 | 704 | 8.26 | 1198 | 1.91 | 14.60 | 32.10 | 11.70 | 25.80 | 88.6 |
| 76 | | 8.91 | 1292 | 1.83 | 14.90 | 32.80 | 11.70 | 25.70 | 95.4 |
| 79 | | 8.09 | 1173 | 1.75 | 14.40 | 31.60 | 11.90 | 26.10 | 84.6 |
| 81 | | 8.56 | 1242 | 2.00 | 14.30 | 31.50 | 12.50 | 27.60 | 86.3 |
| 82 | | 8.61 | 1249 | 2.03 | 14.50 | 31.80 | 12.50 | 27.50 | 87.3 |
| 87 | 705 | 8.22 | 1193 | 1.92 | 14.50 | 31.80 | 12.50 | 27.40 | 83.7 |
| 90 | 705 | 9.14 | 1326 | 2.45 | 14.30 | 31.40 | 13.30 | 29.20 | 92.7 |
| 91 | 705 | 9.16 | 1329 | 2.75 | 14.50 | 32.00 | 13.70 | 30.20 | 93.7 |
| 92 | 704 | 8.76 | 1271 | 1.97 | 14.40 | 31.60 | 11.80 | 25.90 | 93.9 |
| 93 | | 8.78 | 1274 | 2.16 | 14.30 | 31.40 | 13.10 | 26.70 | 93.2 |
| 94 | | 8.69 | 1261 | 2.28 | 13.40 | 29.50 | 12.30 | 27.00 | 92.6 |
| 95 | | 8.32 | 1207 | 2.63 | 14.10 | 31.00 | 12.40 | 27.20 | 97.7 |
| 98 | | 8.27 | 1200 | 2.14 | 14.50 | 31.80 | 11.50 | 25.40 | 91.8 |
| 99 | | 8.36 | 1212 | 2.86 | 14.30 | 31.50 | 12.90 | 28.30 | 92.3 |
| 102 | | 8.62 | 1251 | 1.92 | 12.90 | 28.30 | 11.40 | 25.00 | 95.1 |
| 103 | | 8.61 | 1249 | 2.08 | 11.80 | 25.90 | 11.80 | 25.90 | 93.4 |
| 104 | | 8.61 | 1249 | 2.28 | 12.00 | 26.40 | 12.10 | 26.60 | 92.9 |
| 105 | | 8.55 | 1240 | 2.47 | 12.30 | 27.00 | 12.40 | 27.20 | 92.7 |
| 106 | | 8.57 | 1243 | 2.35 | 12.00 | 26.40 | 12.20 | 26.80 | 92.8 |

^aAll runs were 1.0 s long. ^bAverage for the entire run.

wall. All the chambers had 20 thermocouples evenly spaced at 4 circumferential locations in 5 axial positions. The starred arrows in Fig. 6 indicate that thermocouples are at those axial locations in all the chambers. For the other arrows, the thermocouples are at those axial locations only in the chambers indicated.

The LOX in the coolant passages used a separate feed system from the LOX flowing through the injector. The LOX coolant was countercurrent to the combustion gases and flowed at approximately the same flowrate as the LOX used for combustion.

Test Procedure

The combustion chambers were tested at a nominal chamber pressure of 8.6 MPa (1247 psia) over a mixture ratio (O/F) range of 1.50 to 3.10. Table 2 gives the test conditions for the test series. All the valve sequencing necessary for a repeatable test cycle was programmed into a solid-state timer which was repeatable to within ± 0.001 s. Fuel and oxidizer flows were controlled by fixed-position valves and propellant tank pressure. Coolant inlet pressure was controlled by coolant tank pressure and kept above 13.8 MPa (2000 psia). Coolant exit pressure was kept constant above critical pressure (5.08 MPa) by a closed-loop controller positioning a back pressure valve. The coolant was kept above critical pressure throughout the coolant passages so that two-phase flow did not result. Between runs, the injector was purged to keep the injector clean of dirt. During each test, data are recorded using a transient data acquisition and recording system that records data every .02 s and averages the data over 5 recordings, with the average reported every 0.1 s. The processed data was available in the control room from the mainframe computer within minutes after a test. This access allowed for review of the processed data prior to the next test.

Results and Discussion

Chamber 702 was fired twice. The chamber was inspected after one run and a melted region was detected just upstream of the throat and at the throat. Several oxygen-rich zones were also detected from discoloration of the copper wall and reduction in soot. The zones, which appeared as streaks, began at the injector face and continued past the throat region. The melted region was in line circumferentially with an oxygen-rich streak from the injector but not in line with either machined slot. During the second run, the RP-1 flow decreased, due to a valve malfunction. As a result, the mixture ratio increased from about 2.39 at the beginning of the test to 3.72 at the end, passing through the stoichiometric mixture

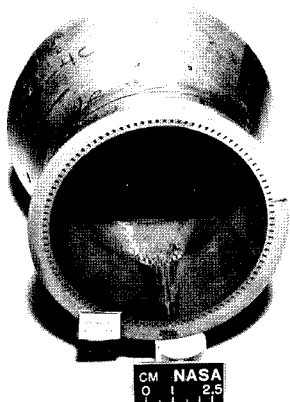


Fig. 7 Chamber 702 throat area.



Fig. 8 Close-up view of machined slot.

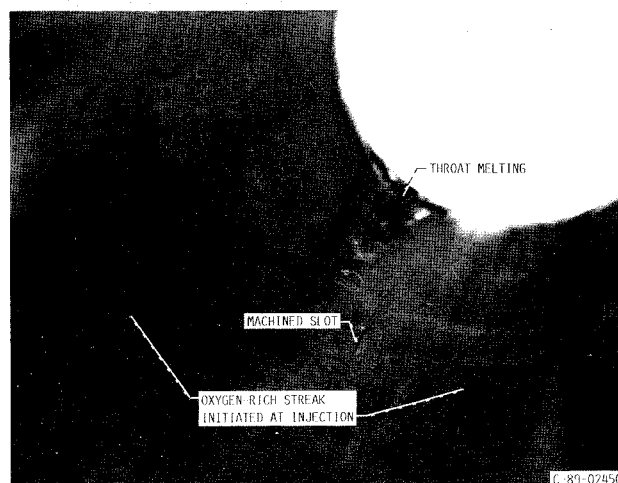


Fig. 9 Chamber 702 after testing.

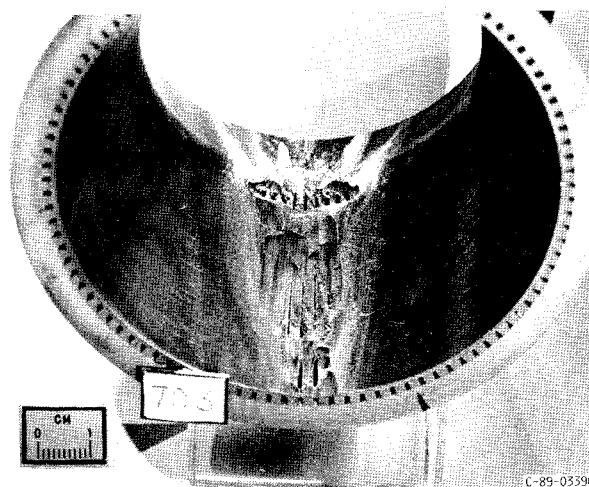


Fig. 10 Chamber 703 throat area.

ratio of 3.43. The chamber was inspected after the second run and there was indication of more melting in the same location, with nine coolant passages opened up (Fig. 7). The injector, injector 288, was not damaged, but in one area, the injector elements were discolored, indicating a hot spot. Chamber 702 was then taken off the test stand and sectioned. Figure 8 shows the slot closest to the melted region. As can be seen, there is no distinguishable effect from the leaking LOX in the region

of the slot. Figure 9 shows the damage to the throat area and upstream of the throat in relation to a machined slot and an oxygen-rich streak.

Six complete runs and one partial run were conducted with chamber 703 and injector 288. After the first three runs, the chamber was inspected and no evidence of damage was detected on the liner surface. The chamber was fired four more times and then inspected again. A part of the chamber liner had melted at the throat and just upstream of the throat (Fig. 10) with 10 cooling channels opened. Several oxygen-rich streaks were also detected from discoloration of the copper wall. The streaks began at the injector face and continued past the throat. The melted region was in line circumferentially with an oxygen-rich streak from the injector but not with either machined slot (Fig. 11). Chamber 703 was then taken off the test stand and also sectioned. Again, there was no distinguishable effect on the chamber from the leaking LOX at the machined slots.

Figure 12 shows the melted region at the throat for the two chambers. The arrows denote the same circumferential location relative to the injector face. As can be seen, the melted regions were not in the same circumferential locations.

Eight complete runs were conducted with chamber 705, which had no machined slots, and injector 288. At this point, the chamber was inspected and small fatigue cracks were detected at the throat. The fatigue cracks were also in line with an oxygen-rich streak. Before further testing, injector 288 was replaced by a new injector, injector 309. Chamber 705 was successfully fired 3 more times with injector 309 and no streaking was detected.

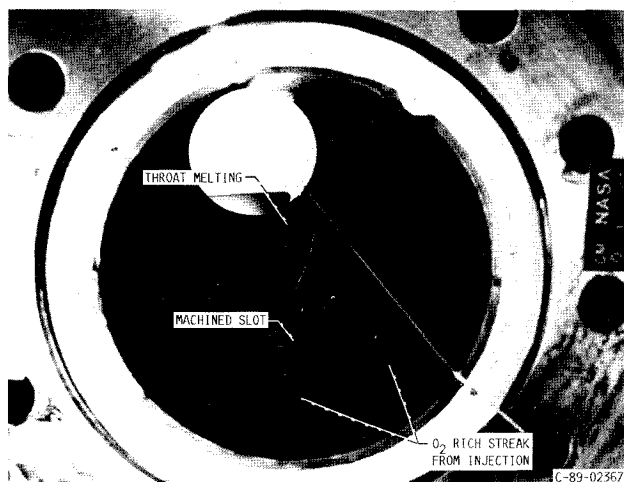


Fig. 11 Chamber 703 after testing.

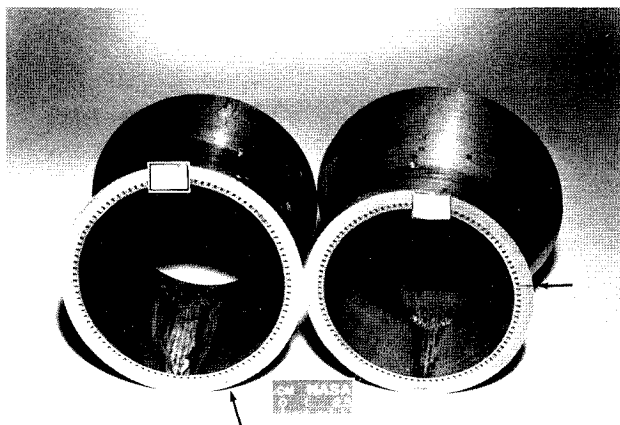


Fig. 12 Melted throat region of both chambers.

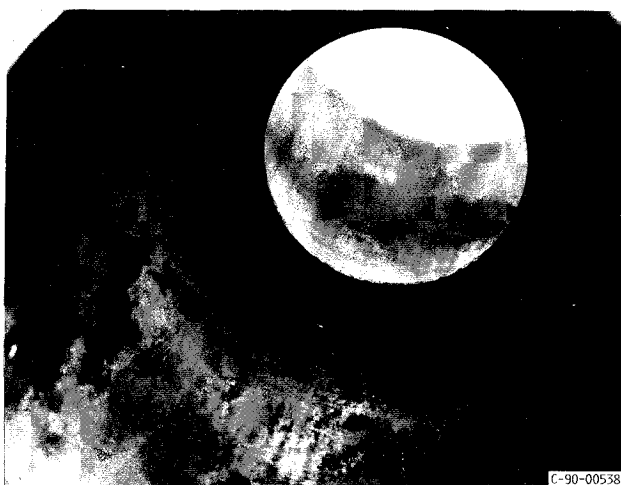


Fig. 13 Throat section of chamber 704 after 20 firings. There is no damage of any kind to the chamber liner.

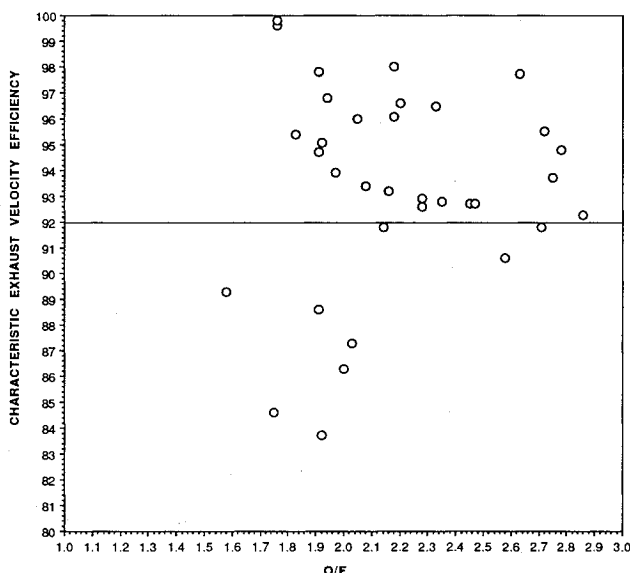


Fig. 14 Characteristic exhaust velocity efficiency as a function of mixture ratio.

Chamber 704, with injector 309, was fired over 20 times, with 16 complete runs. The chamber was inspected periodically during testing and there were no signs of failure or damage to the chamber liner, as shown in Fig. 13. There were no signs of increased temperature directly upstream of the slots as a result of less LOX in the slotted cooling channels (Fig. 5).

During the testing, the chamber walls never reached their ignition temperature and there were no deleterious effects on the chambers as a result of the LOX leaking into the combustion zone. The tests were conducted safely without any damage to the facility or attached hardware.

Injector Performance

Figure 14 is a plot of the C^* efficiency (characteristic exhaust velocity efficiency) versus mixture ratio. The C^* efficiency is the experimental C^* divided by the theoretical C^* , where the theoretical C^* is calculated from the CEC computer program⁸ for the given combustion conditions. The experimental C^* is calculated from

$$C^* = \frac{P_c \cdot A_t \cdot G_e}{\dot{m}_{\text{total}}} \quad (1)$$

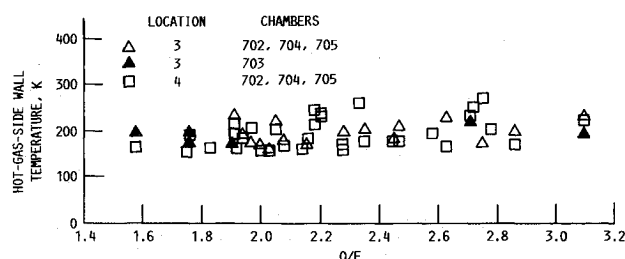


Fig. 15 Hot-gas-side wall temperatures 22.9 cm from the injector.

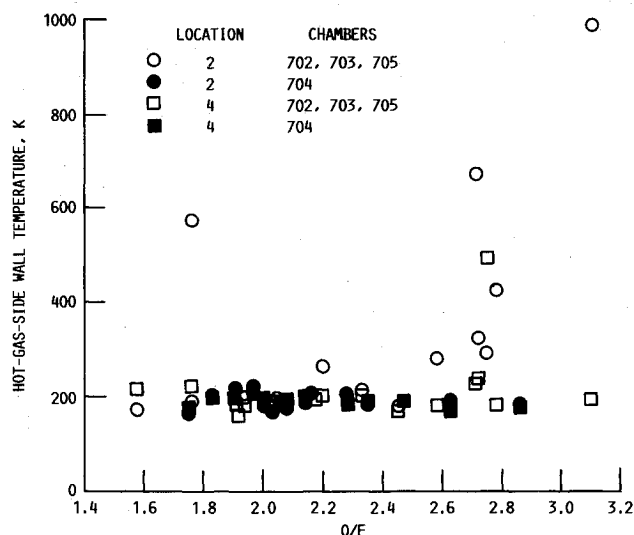


Fig. 16 Hot-gas-side wall temperatures 15.2 cm from the injector.

where P_c is the chamber pressure, A_t is the throat area, G_e is the Earth's gravitational constant, and \dot{m}_{total} is the total propellant mass flow. The 0.5% increase in LOX flow due to the simulated cracks was too small to affect the performance of the chamber and was not included in these calculations. Except for a few anomalies, the C^* efficiency was above 92%, which is acceptable performance for this injector configuration.

Effects of LOX Leaks on Chamber Integrity

Thermocouples were located on the chambers at the slot locations and 2.54 cm (1.0 in.) downstream of the slots to determine the effect of LOX leaks on wall temperature. A one-dimensional analysis was used to determine the hot-gas-side wall temperatures from the thermocouple readings. The wall temperatures downstream of the slots in chamber 703 (16.46 cm upstream of the throat) are compared for the chambers in Fig. 15 which shows similar temperatures for the chambers. In chamber 703, the slots were at locations 1 and 3. The wall temperatures on chamber 703, at slot location 3, are well within the data scatter of the wall temperatures at locations 3 and 4, for those chambers where there were no slots.

The wall temperatures downstream of the slots in chamber 704 (15.24 cm downstream of the injector) are compared for the chambers in Fig. 16. In chamber 704, the slots were at locations 2 and 4. The wall temperatures on chamber 704 were within the data scatter of the other chambers.

The peak temperatures in Fig. 16 indicate a hot spot on the chamber wall. However, the hot spot was not in line with the machined slots, but occurred in line with the oxygen-rich streaks from the injector. Therefore, these results would in-

dicate that the leaking oxygen did not have any effect on the wall temperature directly downstream of the machined slots.

Possible Causes for Chamber Melting

A number of theories have been postulated as to the cause of the melting in the throat region of chambers 702 and 703. The most plausible theories are discussed: blocked coolant passages, coolant maldistribution, combustion instability, the LOX leaking through the machined slots, and injector anomalies. Blocked coolant passages result in localized hot spots. The chambers were sectioned and no blockage was found anywhere. Therefore, blocked coolant passages were not the cause of the melting. A related possible cause is coolant maldistribution since the coolant flows into the chamber through a manifold with only one inlet line. However, the same chamber manifold design had been used in the previous test program (Ref. 6) and with chamber 705 without chamber melting or streaking, indicating even coolant distribution. Hence, coolant maldistribution is not considered to be the cause of the melting.

Another possible cause could be combustion instability although the injector design has a history of stable operation. Generally, high frequency instability would have destroyed all of the hardware, not just the throat, within 0.75 s and our runs included 1 s of steady-state combustion. Hence, combustion instability is not the cause of the melting.

The melting could be a result of LOX leaking through the machined slots upstream of the throat. The oxygen flowing through the slots may have reacted with the chamber wall at the throat, resulting in melting. However, from Fig. 8, one can see that the oxygen leaking from the slot did not react with the wall near the slot. Chamber 704 also had LOX leaking through machined slots upstream of the throat and no melting occurred; the difference between chamber 704 and the melted chambers was the injector and the slot location. Therefore, it was determined that the LOX leaking through the machined slots was not the cause of the melting.

The melting could be from injector anomalies, resulting in an oxygen-rich zone, which appears as a streak, beginning at the injector face and continuing past the throat. The melted regions on both chambers were in line with streaks. The injector, injector 288, was water-flowed tested to detect any injector anomalies, which showed that several of the oxygen element streams did not flow at the proper angle. A new injector, injector 309, was also water-flow tested and all the elements were properly aligned. Chamber 704 was tested with injector 309 and no melting occurred after more than 20 firings.

When considering the effects of the injector anomalies as compared to the LOX leakage through the machined slots, the injector oxygen-rich streaking would be much more detrimental to the chamber than the LOX leakage. The direction of flow out of the cracks is perpendicular to the main combustion stream so the LOX would tend to get dispersed. Since it is unlikely to reach the opposite side of the chamber, the stream from the slots would only damage the chamber wall near the slots. However, there was no damage near the slots and no significant temperature rise. The direction of flow from the injector elements is relatively parallel to the main combustion stream, even for misaligned injector elements, and, therefore, the oxygen stream is less likely to be dispersed. A misaligned injector element could easily impinge on the chamber wall, causing streaking. Approximately 1% of the injected oxygen flows through each hole. If 3 or 4 holes are misaligned, 3 or 4% of the total oxygen would be impinging on the chamber wall, as compared to 0.25% of the oxygen coolant leaking through one of the machined slots. This analysis would indicate that the melting in the previous test series was due to the injector and not the oxygen leaking into the chamber from the cooling channels.

Summary of Results

Four OFHC copper thrust chambers with identical geometry were tested with LOX and RP-1 as propellants and LOX as the coolant at a nominal chamber pressure of 8.6 MPa (1247 psia) over a mixture ratio (O/F) range of 1.5 to 3.10. To determine the effect of leaking LOX upstream of the throat, the thrust chambers were fabricated with slots machined between the cooling passage wall and the hot-gas side wall, to simulate cracks. The results of these tests are as follows:

1) LOX leaking into the combustion zone through simulated fatigue cracks (machined slots) did not have a deleterious effect on the thrust chambers in the regions of the slots, nor did the wall of the chambers reach its ignition temperature at any location.

2) The wall temperature measurements did not indicate any increase in temperature just downstream of the slots.

3) There was melting in the throat region of chambers 702 and 703; however, the melting was not in line with the machined slots. The cause of the melting was determined to be injector anomalies which resulted in oxygen-rich zones, which appear as streaks, beginning at the injector face and continuing past the throat.

4) The results of these tests indicated that LOX can be used safely as a coolant, even if cracks should develop in the chamber wall upstream of the throat.

References

¹Luscher, W. P., and Mellish, J. A., "Advanced High Pressure Engine Study for Mixed-Mode Vehicle Applications," NASA CR-135141, January 1977.

²Caluori, V. A., Conrad, R. T., and Jenkins, J. C., "Technology Requirements for Future Earth-to-Geosynchronous Orbit Transportation Systems," NASA CR-3265, April 1980.

³Rosenberg, S. D., and Gage, M. L., "Compatibility of Hydrocarbon Fuels with Booster Engine Combustion Chamber Liners," AIAA/ASME/ASME/SAE 24th Joint Propulsion Conference, AIAA Paper 88-3215, Boston, MA, July 1988.

⁴Rousar, D. C., and Miller, F., "Cooling with Supercritical Oxygen," AIAA Paper 75-1248, AIAA/SAE 11th Propulsion Conference, Anaheim, CA, September 1975.

⁵Price, H. G., "Cooling of High-Pressure Rocket Thrust Chambers with Liquid Oxygen," *Journal of Spacecraft and Rockets*, Vol. 18, No. 4, 1980, pp. 338-343.

⁶Price, H. G., and Masters, P. A., "Liquid Oxygen Cooling of High Pressure LOX/Hydrocarbon Rocket Thrust Chambers," NASA TM-88805, August 1986.

⁷Dederra, H., and Kirner, E., "High Pressure Rocket Engine Liquid Oxygen Technology," XXXVII Congress of the International Astronautical Federation, IAF-76-174, Anaheim, CA, October 1976.

⁸Gordon, S., and McBride, B. J., "Computer Program for Calculation of Complex Equilibrium Compositions, Rocket Performance, Incident and Reflected Shocks, and Chapman-Jouguet Detonations," NASA SP-273, Interim Revision, March 1976.

Dynamics of Reactive Systems, Part I: Flames and Part II: Heterogeneous Combustion and Applications and Dynamics of Explosions

A.L. Kuhl, J.R. Bowen, J.C. Leyer, A. Borisov, editors

Companion volumes, these books embrace the topics of explosions, detonations, shock phenomena, and reactive flow. In addition, they cover the gasdynamic aspect of nonsteady flow in combustion systems, the fluid-mechanical aspects of combustion (with particular emphasis on the effects of turbulence), and diagnostic techniques used to study combustion phenomena.

Dynamics of Explosions (V-114) primarily concerns the interrelationship between the rate processes of energy deposition in a compressible medium and the concurrent nonsteady flow as it typically occurs in explosion phenomena. *Dynamics of Reactive Systems (V-113)* spans a broader area, encompassing the processes coupling the dynamics of fluid flow and molecular transformations in reactive media, occurring in any combustion system.

To Order, Write, Phone, or FAX:



American Institute of Aeronautics and Astronautics
c/o TASC0
9 Jay Gould Ct., P.O. Box 753, Waldorf, MD 20604
Phone (301) 645-5643 Dept. 415 FAX (301) 843-0159

V-113 1988 865 pp., 2-vols. Hardback
ISBN 0-930403-46-0
AIAA Members \$92.95
Nonmembers \$135.00

V-114 1988 540 pp. Hardback
ISBN 0-930403-47-9
AIAA Members \$54.95
Nonmembers \$92.95

Postage and Handling \$4.75 for 1-4 books (call for rates for higher quantities). Sales tax: CA residents add 7%, DC residents add 6%. All orders under \$50 must be prepaid. All foreign orders must be prepaid. Please allow 4 weeks for delivery. Prices are subject to change without notice.